Available online at www.sciencedirect.com
SCIENCE DIRECT®
Journal of Solid State Chemistry 170 (2003) 330–338
JOURNAL OF SOLID STATE CHEMISTRY
http://elsevier.com/locate/jssc

A new ternary cadmium–zirconium–sodium oxalate with an open framework: crystal structure, solid-state NMR spectroscopy and thermal behavior

E. Jeanneau,[a] N. Audebrand,[a] M. Le Floch,[b] B. Bureau,[b] and D. Louër[a,*]

[a] *Laboratoire de Chimie du Solide et Inorganique Moléculaire (UMR 6511 CNRS), Institut de Chimie, Université de Rennes, Avenue du Général Leclerc, 35042 Rennes Cedex, France*

[b] *Laboratoire Verres et Céramiques (UMR 6512 CNRS), Institut de Chimie, Université de Rennes, Avenue du Général Leclerc, 35042 Rennes Cedex, France*

Received 31 July 2002; received in revised form 26 September 2002; accepted 5 October 2002

Abstract

A mixed cadmium-zirconium-sodium oxalate with an open architecture has been synthesized from precipitation methods at ambient pressure. It crystallizes in an hexagonal system, space group $P6_422$ (no. 181), $a = 8.793(1)$ Å, $c = 24.530(1)$ Å, $V = 1642.5(3)$ Å^3 and $Z = 3$. The structure displays a $[CdZr(C_2O_4)_4]^{2-}$ helicoidal framework. It is built from CdO_8 and ZrO_8 square-based antiprisms connected through bichelating oxalates and displays channels along different directions. The sodium counter-cations are located inside the voids of the structure together with water molecules. They exhibit a dynamic disorder which has been further investigated by ^{1}H and ^{23}Na solid-state NMR. The study pointed out two types of water molecules and sodium atoms, with a high mobility for one of each. The thermal decomposition has been studied in situ by temperature-dependent X-ray diffraction and thermogravimety. The final product is a mixture of cadmium oxide, zirconium oxide and amorphous sodium carbonate.

Keywords: Cadmium–zirconium–sodium oxalate; Single-crystal diffraction; Crystal structure; ^{1}H solid-state NMR; ^{23}Na solid-state NMR; Open framework; Porous material; Building units; Thermal decomposition; Temperature-dependent powder diffraction

1. Introduction

There has been an intense activity on the synthesis and structural design of open-framework materials, from which the concepts of building unit and net connectivity have been extensively discussed (see, for example, Refs. [1,2] and references therein). Recent studies on mixed cadmium–zirconium oxalates have demonstrated the possibility to conceive various structural arrangements [3–5]. Indeed, the crystal structures of the reported phases are built from basic units MO_8 ($M = Cd, Zr$) connected by bichelating oxalate groups. Two structure types have been reported and the relationships with open-framework structures based on mixed MO_8 polyhedra have been discussed [5]. The structures consist both of chemically identical $[CdZr(C_2O_4)_4]^{2-}$ anionic groups forming two different nanoporous frameworks, whose topology originates from the two frequent configurations dominating the stereochemistry of eight-fold coordination, i.e., the dodecahedron and the square antiprism [6,7]. With dodecahedra, the structure is built from a net of perpendicular zigzag chains with a (–Cd–oxalate–Zr–oxalate–)$_\infty$ sequence and exhibits tunnels with square cross sections. Representative examples with counter-cations adopting also an eight-fold coordination are $Cd_2Zr(C_2O_4)_4 \cdot 6H_2O$ [3] and $CdZrK_2(C_2O_4)_4 \cdot 8H_2O$ [5], in which the anionic framework is counterbalanced by one Cd^{2+} or two K^+ cations, respectively, located in the voids of the structures. The topology of the anionic framework based on square antiprism polyhedra presents a hexagonal symmetry and is built from interconnected helical chains exhibiting a sequence similar to that found in the zigzag chains. The cations located inside the channels parallel to the *c*-axis counterbalance the anionic framework. This structure has been reported for two compounds with cations exhibiting different

*Corresponding author. Fax: +33-2-99-38-34-87.
E-mail address: Daniel.Louer@univ-rennesl.fr (D. Louër).

0022-4596/03/$ - see front matter © 2002 Elsevier Science (USA). All rights reserved.
doi:10.1016/S0022-4596(02)00100-7

charges, namely the ammonium cation NH_4^+ in $CdZr(NH_4)_2(C_2O_4)_4 \cdot 3.9H_2O$ and the protonated ethylenediamine cation $[NH_3–(CH_2)_2–NH_3]^{2+}$ in $CdZr(C_2N_2H_{10})(C_2O_4)_4 \cdot 4.4H_2O$ [4]. In this last structure, the counterbalancing organic cations, located in tunnels with a hexagonal cross section, clearly cannot be discussed in terms of coordination polyhedra. It is then of interest to consider the extension of this series of cadmium–zirconium–oxalate compounds to elements known for presenting a flexible coordination, such as sodium whose coordination number ranges from four to nine [8]. The question is thus to know if the resulting material adopts the structure with tunnels having a square cross section, like the related potassium phase, or a hexagonal cross section. The present study deals with the synthesis of the sodium-based compound, its structure determination from single-crystal X-ray diffraction data, ^1H and ^{23}Na NMR spectroscopy, as well as its thermal behavior.

2. Experimental

2.1. Preparation and preliminary characterization

Crystals of mixed cadmium–zirconium–sodium oxalate $CdZrNa_2(C_2O_4)_4 \cdot 8.5H_2O$ were obtained by a soft chemistry route. The title compound was synthesized from a mixture of 0.50 g of cadmium nitrate $Cd(NO_3)_2 \cdot 4H_2O$ (Merck) and 0.37 g of zirconium dinitrate oxide from Alpha Aesar (whose chemical formula is $Zr(OH)_2(NO_3)_2 \cdot (1+x)H_2O$ [9]) in 50 ml of deionized water. The solution was stirred until complete dissolution and then titrated by a 0.1 mol l^{-1} oxalic acid solution in excess until a white precipitate was formed. The solution was heated up to 60°C and ~ 2 ml of NaOH was slowly poured in, still under stirring. Finally, ~3 ml of concentrated HNO_3 was slowly added until complete dissolution. The evaporation of the solution at room temperature led to the formation of bipyramidal-shaped transparent crystals of average size 100 μm. The crystals were filtered, washed with deionized water, ethanol and dried under air. Powder X-ray diffraction patterns of the powdered crystals, obtained with a Siemens D500 diffractometer ($\lambda = 1.5406$ Å) indicated that the product was a pure new material. It was subsequently verified that the powder data were indexed by the structural results reported in the present study. The chemical formula was derived from energy dispersive spectrometry (ratio Cd/Zr/Na = 1/1/2), performed using a JSM 6400 spectrometer equipped with an Oxford Link Isis analyzer and from the crystal structure determination reported below. It corresponds to the chemical composition $CdZrNa_2(C_2O_4)_4 \cdot 8.5H_2O$. Assuming this formula, the yield found for this synthesis is 52%. The images made by means of a JEOL JSM-6301 F Scanning Electron Microscope (SEM) are shown in Fig. 1. From the magnified image, an etching pattern on the surface of the crystals can be observed. This feature can likely be explained by the use of concentrated nitric acid in the course of the synthesis. The particular geometry of such etching patterns is generally related to the crystalline structure and surface defects of the product [10]. Such feature was already observed with related materials such as $CdZr(NH_4)_2(C_2O_4)_4 \cdot 4H_2O$ [4] and $CdZrK_2(C_2O_4)_4 \cdot 8H_2O$ [5], which were obtained through similar synthetic routes.

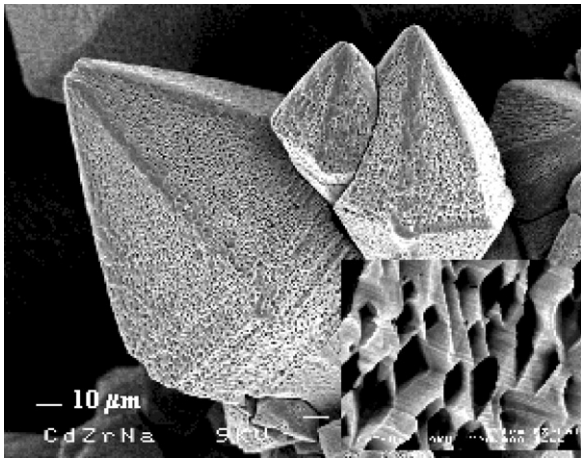

Fig. 1. SEM micrograph displaying bipyramidal shaped crystals of $CdZrNa_2(C_2O_4)_4 \cdot 8.5H_2O$. The close-up on the bottom right shows the typical etching pattern found on the surface of the crystals.

2.2. Thermal analysis

Thermogravimetric analysis (TG) was carried out with a Rigaku Thermoflex instrument. The powdered samples were spread evenly in large platinum crucibles to avoid mass effects. Temperature-dependent X-ray diffraction (TDXD) was performed under dynamic air with a powder diffractometer combining the curved-position-sensitive (PSD) from INEL (CPS 120) and a high-temperature attachment from Rigaku. The detector was used in a semi-focusing arrangement by reflection ($CuK\alpha_1$ radiation) as described elsewhere [11].

2.3. NMR measurements

The spectra were recorded at room temperature on an ASX 300 Bruker spectrometer operating at 300 MHz for ^1H ($I = 1/2$) and 79.39 MHz for ^{23}Na ($I = 3/2$) with a 4 mm MAS probe spinning up to 15 kHz. A single-pulse excitation was used to acquire the signal. The pulse duration was 3 μs for ^1H, whereas for ^{23}Na it was chosen equal to 1 μs in order to fulfill the condition $\nu_{rf} < \nu_Q$ that avoids any line distortion due to quadrupolar effects [12]. For ^{23}Na spectra, $NaNO_3$ dissolved in water

was used as reference (0 ppm). The recycle delay effect between two scans was checked to ensure that no contribution was favored, especially for ^{1}H spectra. Finally, it was set to 1 s for both ^{1}H and ^{23}Na nuclei. The simulations of the experimental spectra were performed using the Dm2000nt version of the Winfit software [13].

2.4. Single-crystal diffraction data collection

A suitable single crystal of linear dimensions $0.19 \times 0.13 \times 0.12$ mm was carefully selected. Intensity data were collected on a four-circle Nonius Kappa CCD diffractometer equipped with a CCD area detector, using the Mo$K\alpha$ radiation ($\lambda = 0.71073$ Å), through the program COLLECT [14]. Lorentz-polarization factor correction, peak integration and background determination were carried out with the program DENZO [15]. Frame scaling and unit-cell parameters refinement were made with the program SCALEPACK [15]. Numerical absorption correction was performed by modeling the crystal faces using NUMABS [16]. The resulting set of hkl reflections was used for structure refinement. Crystallographic data and details on data collection and refinement are listed in Table 1. Structure drawings were carried out with Diamond 2.1e, supplied by Crystal Impact (Brandenburg, 2001) [17].

Table 1
Crystallographic data and structure refinement parameters for $CdZrNa_2(C_2O_4)_4 \cdot 8.5H_2O$

Empirical formula	$CdZrNa_2C_8O_{24.5}H_{17}$
Crystal system	Hexagonal
Space group	$P6_422$ (No. 181)
Crystal size (mm)	0.19 × 0.13 × 0.12
a (Å)	8.793(1)
c (Å)	24.530(1)
Volume (Å^3)	1642.5(3)
Z	3
Formula weight (g mol^{-1})	754.82
ρ_{calc} (g cm^{-3})	2.289
λ (Mo$K\alpha$) (Å)	0.71073
θ range (deg)	3.15–34.96
Index ranges	$-13 \leqslant h \leqslant 14$, $-14 \leqslant k \leqslant 14$, $-39 \leqslant l \leqslant 37$
Unique data	2377
Observed data ($I > 2\sigma(I)$)	2010
R_1 ($I > 2\sigma(I)$)	0.098
R_1 (All)	0.109
ωR_2 ($I > 2\sigma(I)$)	0.297
ωR_2 (All)	0.309
Refinement method	Full-matrix least-squares on $\lvert F^2 \rvert$
Goodness of fit	1.101
No. of variables	84
No. of restraints[a]	1
Largest difference map peak and hole (e Å^{-3})	3.086 and –2.556

[a] C2–O2 distance restrained to be equal to 1.25(1) Å.

3. Results and discussion

3.1. Structure solution

The structure was solved with the hexagonal symmetry, space group $P6_422$. The heavy atoms were located using the direct methods by means of the program SIR97 [18]. The remaining atoms, constitutive of the porous anionic framework, $[CdZr(C_2O_4)_4]^{2-}$ described below, were found from successive Fourier difference map analyses with SHELXL97 [19]. The two sodium atoms (Na1 and Na2) were localized near a 6_4-fold axis and were thus constrained to lie along this axis in the tunnels of the framework. The localization of one of the water molecules was more laborious. Indeed, Fourier map analyses showed a quasi-continuous electron density around the sodium atoms. This feature could correspond to either a statistical occupancy of water molecules from one channel to another or to the presence of less bonded water molecules displaying dynamic properties. It is worth noting that such feature was expected from the diffuse scattering between diffraction peaks observed in the reciprocal planes perpendicular to the c*-axis. The oxygen atom Ow1 was thus located on the maximum density peaks and its atomic displacement parameter was refined anisotropically. The result can be seen in Fig. 2, which shows the sodium atoms together with the surrounding oxygen atoms Ow1 displaying marked anisotropic thermal motion probability ellipsoids. It can be seen that Ow1 displays a huge motion leading to a 'quasi-continuous' helicoidal trace. To overcome this feature, the atomic displacement parameter U_{eq} of Ow1 was fixed in the last stages of the refinement to the isotropic value 0.08 Å^2, as usually found in related materials [3]. However, it must be noted that the disorder of Ow1 is a real structural feature of the compound, which needs further investigation. This is discussed in detail below from an NMR spectrometry study. The last cycles of the structure refinement included atomic positions and anisotropic atomic displacement parameters for all atoms, except Ow1. The site-occupancy factor for Ow1 and Ow2 were 1.0 and 0.5, respectively, while the site-occupancy factor for Ow3 converged to 0.63(5), i.e., 8.5 ± 0.2 water molecules per chemical formula. The final atomic coordinates are given in Table 2 and selected bond distances and angles in Table 3.

3.2. Description of the structure

The compound $CdZrNa_2(C_2O_4)_4 \cdot 8.5H_2O$ displays a three-dimensional arrangement of eight-fold cadmium and zirconium polyhedra linked through oxalate groups. The structure is related to that of $CdZr(NH_4)_2(C_2O_4)_4 \cdot 3.9H_2O$ and also shows similarities with that

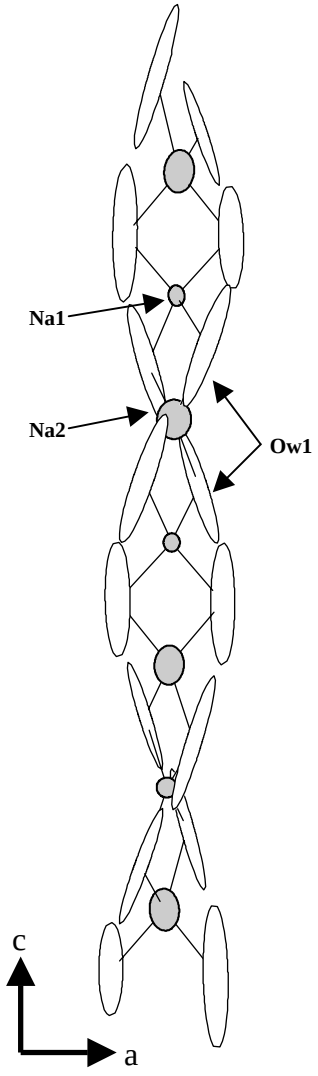

Fig. 2. View of the sodium atoms and their surrounding oxygen atom Ow1 showing the tendency of the electron density delocalization. Displacement ellipsoids are plotted at the 50% probability level.

Table 2
Positional and equivalent isotropic atomic displacement parameters with their standard deviations for $CdZrNa_2(C_2O_4)_4 \cdot 8.5H_2O$

Atom	x	y	z	U_{eq}/U_{iso} (Å^2)
Cd	1/2	1/2	2/3	0.0223(3)
Zr	0	1/2	5/6	0.0240(3)
Na1	0	0	5/6	0.038(1)
Na2	0	0	2/3	0.130(7)
O1	0.564(1)	0.306(1)	0.7236(4)	0.058(2)
O2	0.9111(9)	0.6580(9)	0.7866(3)	0.043(2)
O3	0.741(1)	0.6602(9)	0.7195(3)	0.047(2)
O4	0.768(1)	0.3167(9)	0.7809(3)	0.050(2)
C1	0.703(1)	0.383(1)	0.7505(3)	0.031(1)
C2	0.789(9)	0.584(1)	0.7517(3)	0.036(2)
Ow1	0.206(2)	0.019(2)	0.7559(4)	0.080[a]
Ow2	1/2	1/2	0.8339(6)	0.062(4)
Ow3	0	1/2	0.6674(6)	0.080(5)

[a] Fixed isotropic value. $U_{eq} = (1/3)\sum_i \sum_j U_{ij} a_i^* a_j^* \boldsymbol{a_i} \boldsymbol{a_j}$

Table 3
Selected interatomic distances (Å) and bond angles (deg) for $CdZrNa_2(C_2O_4)_4 \cdot 8.5H_2O$

*MO*8 square-based antiprisms			
CdO_8			
		s	
Cd–O1, O1$^{i, ii, iii}$	2.476(9)	O1–O3 (x 4)	2.70(1)
Cd–O3, O3$^{i, ii, iii}$	2.270(7)	O1–O3^{i} (x 4)	2.84(1)
		l	
		O1–O1^{ii} (x 2)	3.02(2)
		O3–O3^{iii} (x 2)	2.86(1)
		O1–O3^{ii} (x 4)	3.24(1)
ZrO_8			
		s	
Zr–O2, O2$^{iv, v, vi}$	2.223(7)	O2–O4 (x 4)	2.62(1)
Zr–O4, O4^{iv,v,vi}	2.263(8)	O2–O4^{vi} (x 4)	2.72(1)
		l	
		O2–O2^{v} (x 2)	2.66(1)
		O4–O4^{iv} (x 2)	2.83(2)
		O2–O4^{iv} (x 4)	2.92(1)
Oxalate Anion			
C1–C2	1.54(1)	O1–C1–C2	114.4(7)
C1–O1	1.25(1)	O4–C1–C2	116.8(7)
C1–O4	1.25(1)	O1–C1–O4	128.2(9)
C2–O2	1.270(9)	O3–C2–C1	120.4(7)
C2–O3	1.239(5)	O2–C2–C1	113.7(6)
		O2–C2–O3	125.8(9)

Symmetry codes: (i) $1-x,1-y,z$; (ii) $1-y,1-x,\frac{4}{3}-z$; (iii) $y,x,\frac{4}{3}-z$; (iv) $x,x-y,\frac{5}{3}-z$; (v) $2-x,1-x+y,\frac{5}{3}-z$; (vi) $2-x,1-y,z$.

of $CdZr(C_2N_2H_{10})(C_2O_4)_4 \cdot 4.4H_2O$ [4]. The coordination polyhedra of both the zirconium and cadmium atoms (Fig. 3) can be described as slightly distorted square antiprisms similar to those found, for instance, in $Pb_2Zr(C_2O_4)_4 \cdot nH_2O$ [20]. The two edge lengths l and s are reported in Table 3, according to Hoard and Silverton's formalism [6]. While the eight s distances are fairly equivalent, the l values show a discrepancy with three different values. This feature is linked to the distortion of the polyhedra with a tilt angle of 30° between the two bases, instead of the 45° angle found in the ideal square-based antiprism. Moreover, the mean square planes of the polyhedra's bases are strictly parallel with respect to each other for both ZrO_8 and CdO_8 polyhedra. Within the ZrO_8 antiprism, the mean Zr–O distance [2.243(8) Å] agrees with the expected value (2.184 Å) calculated with the bond valence method using the program VALENCE [21]. The standard mean deviation from planarity of the zirconium antiprism bases is 0.07 Å for the two bases. Within the CdO_8 antiprism, the mean Cd–O distance [2.373(8) Å] is close to the expected value (2.414 Å) obtained from the bond valence method for an eight-fold cadmium atom. The mean standard deviation from planarity of the two square bases is 0.05 Å.

There is only one crystallographic chelating oxalate group in the structure of $CdZrNa_2(C_2O_4)_4 \cdot 8.5H_2O$. It spans half of the *s* edges of each heavy atom polyhedra (Fig. 3). The bond distances and angles within the oxalate group are listed in Table 3. They are in good agreement with the mean values reported by Hahn [22] for a number of oxalate compounds, i.e. 1.24 Å, 1.55 Å, 117° and 126° for C–O and C–C bond lengths, O–C–C and O–C–O angles, respectively. This oxalate group is close to planarity with a mean atomic deviation from the least-square plane of 0.07 Å.

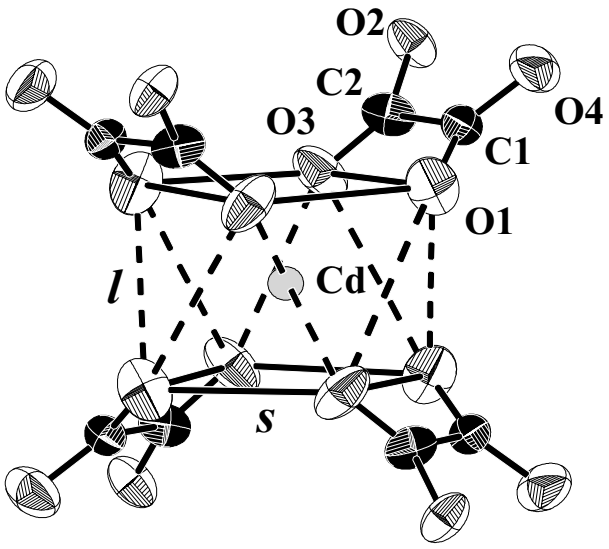

Fig. 3. Representation of the cadmium coordination polyhedron. The O–O distances are indicated according to the common notation used by Hoard and Silverton [6]. The zirconium environment is similar to that of cadmium.

The three-dimensional structure can be described as a combination of a porous $[CdZr(C_2O_4)_4]^{2-}$ anionic framework, counter-cations ($2Na^+$) and water molecules. The anionic skeleton is formed by CdO_8 and ZrO_8 square-based antiprisms linked together through chelating oxalate groups. The distorted antiprisms, with bases making an angle of 30°, are linked together to form an helical wire. These right-hand helices (Fig. 4a) consist of alternating cadmium and zirconium atoms linked through the oxalate groups, leading to the formation of $(–Cd–oxalate–Zr–oxalate–)_\infty$ chains along the *c*-axis. The period of a helix is constituted of three cadmium polyhedra, three zirconium polyhedra and six oxalate groups. The entire structure framework consists of a three-dimensional network of interconnected helices, as described in detail in Ref. [2]. The resulting open-framework $[CdZr(C_2O_4)_4]^{2-}$ displays tunnels along the three crystallographic axes and [1 1 0]. The tunnels along [001] have a hexagonal cross section with a $\sim$4.5 Å diameter (Fig. 4b). The projections along [110], [100] and [010] display two kinds of tunnels: one with a square cross section of $\sim$ 4.5 Å side and one with a $\sim 4.5 \times 10$ Å ellipsoidal cross section (Fig. 4a). Solvent accessible voids have been calculated by means of the program SOLV included in the software PLATON [23]. The total volume within the anionic framework available for guest water molecules and Na cations is 790 $Å^3$, which corresponds to approximately 48% of the total unit-cell volume.

The charge balance is achieved by the alternating Na1 and Na2 cations located in the tunnels with a hexagonal cross section (Fig. 4b). The distance between two successive sodium atoms is $c/6$ [4.09(2) Å]. The environment of the sodium atoms cannot be described

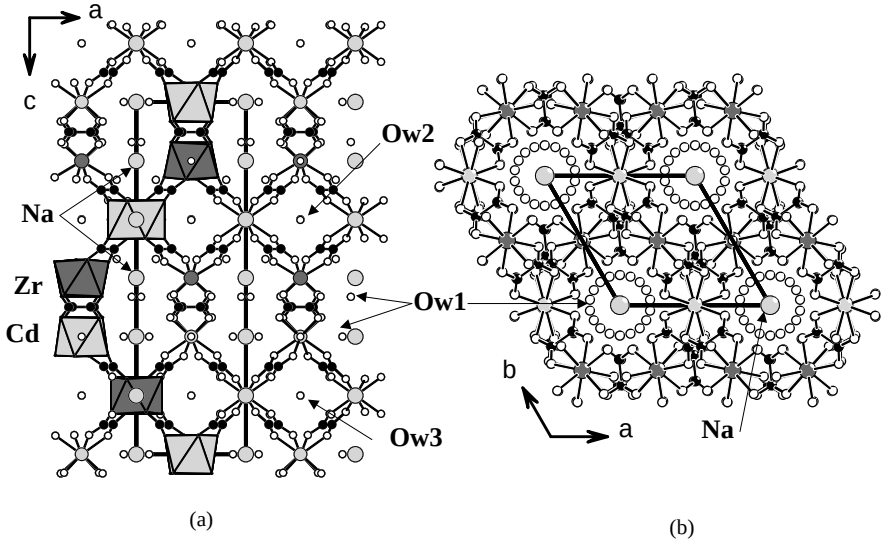

Fig. 4. Projection of the structure of $CdZrNa_2(C_2O_4)_4 \cdot 8.5H_2O$ along (a) the *b*-axis and (b) the *c*-axis. The polyhedral representation (CdO_8: light gray; ZrO_8: dark gray) shows an helix over one period.

accurately from the X-ray diffraction data because of the dynamic disorder discussed above and further in the next section. However, the sodium coordination polyhedra can be considered to be formed of eight oxygen atoms adopting a highly distorted bicapped trigonal prism arrangement. For both sodium atoms, four long Na–O distances are observed between Na and O atoms belonging to oxalate groups from the anionic framework [2.936(8) Å and 2.999(8) Å for Na1–O2 and Na2–O3]. The other distances are shorter bonds with the disordered oxygen atom [2.57(1) and 2.80(1) Å for Na1–Ow1 and Na2–Ow1]. The two polyhedra possess a common edge, thus forming infinite chains along the *c*-axis (Fig. 2). Another worth noting feature is the fact that Na2 has an unexpected large thermal motion compared to that of Na1.

The channels are also filled by two types of water molecules (Fig. 4a). The first type consists of the high-motion water molecule Ow1 in the sodium environment. The two other water molecules that are not bonded to a metal atom, Ow2 and Ow3, probably form weak hydrogen bonds with their nearest oxygen atom from the anionic framework [Ow2−O4 = 2.89(1) Å, Ow3−O1 = 2.84(1) Å].

3.3. NMR results

^{1}H NMR: Fig. 5 shows the proton static spectrum of the powdered sample. Two Lorentzian contributions with equal integrated intensities are necessary to account for the line shape, which point out that two kinds of proton are present in the compound. They have identical positions, within the experimental uncertainty, whereas their line widths are very different. These results are consistent with the description of the structure reported in the previous section since all protons belong to water molecules. Consequently, the sharper contribution ($\Delta\nu_{1/2} = 1863$ Hz) was attributed to mobile water molecules and the larger one ($\Delta\nu_{1/2} = 9167$ Hz) to molecules more bounded to the framework. Note that this broad line width value is still far from a rigid lattice value for water molecules [24].

^{23}Na NMR: The solid-state NMR analysis of quadrupolar nuclei such as ^{23}Na is more complicated because two major interactions contribute to the shape of the powder spectrum: the chemical shift anisotropy (CSA) and the quadrupolar effect. According to the X-ray structural results, were two kinds of Na atoms detected, the NMR spectra should then be the sum of two contributions with an axial symmetry, due to the six-fold axis of the Na sites, if not averaged by motion. In agreement with this description, the following interpretation of the recorded spectra is proposed.

The MAS spectrum recorded at a rate of 5 kHz shown in Fig. 6 exhibits a slightly asymmetric line shape. As the MAS technique simultaneously reduces the dipolar and quadrupolar interactions and averages the chemical shift anisotropy, it appears that the only convenient way to give account of the MAS line is to use two narrow and symmetric Lorentzian contributions (Fig. 6). The parameters which enable to reach the best fit are given in Table 4. The isotropic chemical shifts assigned to both sodium atom types are relatively close to each other (−15.4 and −18.8 ppm) evidencing that Na1 and Na2 have similar mean neighborhoods. Moreover, the

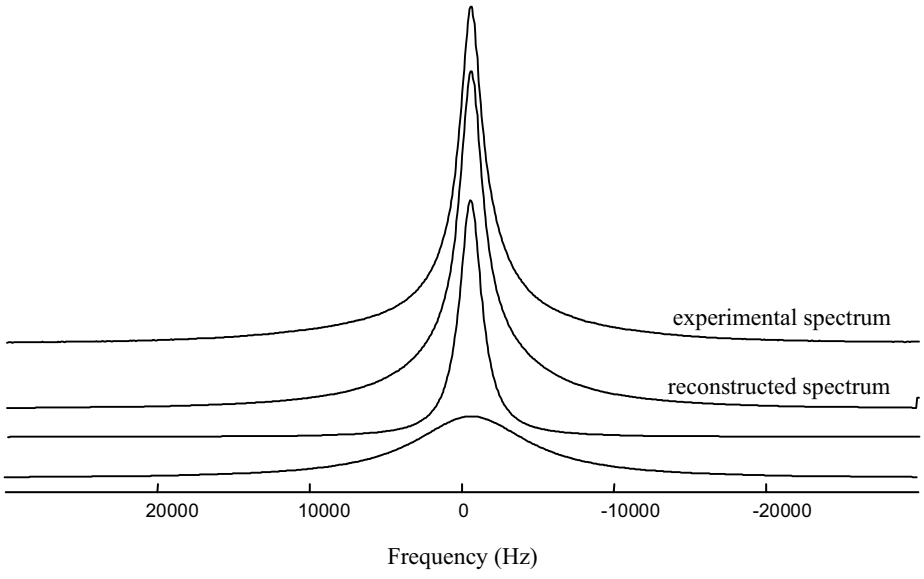

Fig. 5. ^{1}H static spectrum showing two behaviors for water molecules. (The two lower curves are the two components used in the reconstructed spectrum.)

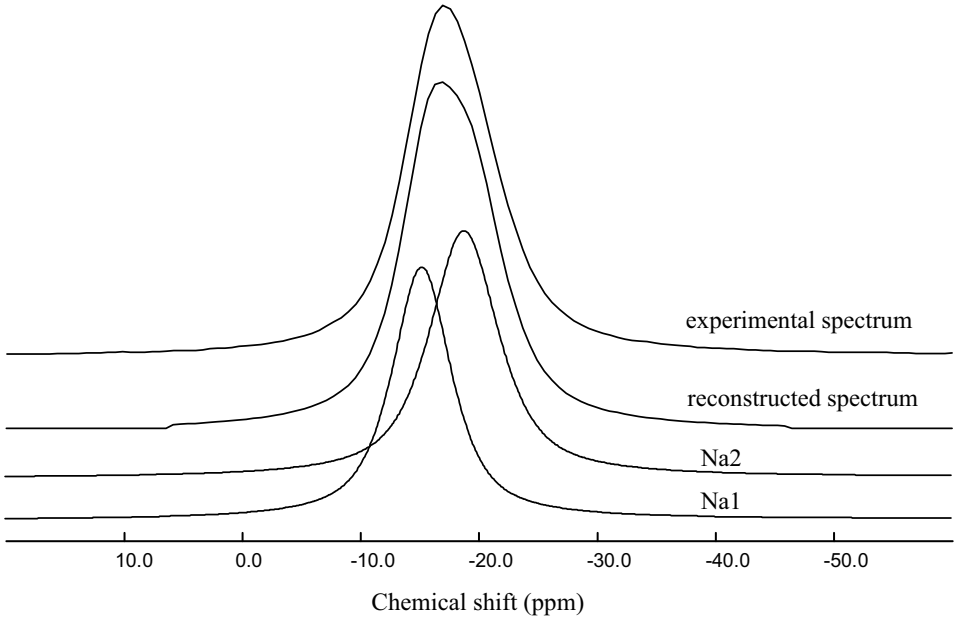

Fig. 6. ^{23}Na MAS spectrum (5 kHz) evidencing two Lorentzian contributions labeled Na1 and Na2.

Table 4
Parameters used for the reconstruction of the ^{23}Na NMR static and MAS (5 kHz) spectra. A CSA model was used for Na1 static line and pure Lorentzians for all other contributions

	Line	Static		MAS
Isotropic chemical shift	Na1	−14.3		−15.4
(± 1 ppm)	Na2	−19.4		−18.8
		δ	η	
Chemical shift anisotropy	Na1	26.6	0.18	—
(± 1 ppm)	Na2	—		—
Lorentzian widths	Na1	—		500
(± 50 Hz)	Na2	880		550
Integrated intensities	Na1	46		50
(± 5%)	Na2	54		50

integrated intensity values confirm that the two types of sodium atoms are found in equal quantities.

The static spectrum reconstruction is much more complex since all NMR interaction types contribute to the line shape. It was impossible to give account for this spectrum using a quadrupolar line shape model. Moreover, no spinning side bands due to external transitions, and characteristic of quadrupolar effects, are visible on the MAS spectrum. Then, as shown in Fig. 7, the ^{23}Na NMR static spectrum can be convincingly reconstructed with two contributions having equal integrated intensities and centered on the same isotropic chemical shift previously obtained from the MAS result (Table 4). For the first contribution, a CSA model is used with a weak anisotropy $\delta = 26.63$ ppm and a low asymmetry factor $\eta = 0.18$, indicating the existence of a sodium atom on a high symmetry site with a preferential direction. The second contribution is a narrow Lorentzian component, which may account for a mobile sodium atom.

The quality of the fits together with the full agreement between the parameters used for both reconstructions, static and MAS, confirmed the validity of the assumptions done consisting in attributing the static line shape to CSA rather than to quadrupolar interaction. Overall, these results lead us to consider the existence of two different kinds of sodium atoms in equal quantity. The first one exhibits a weak axial CSA in full agreement with its position on the six-fold axis as expected from X-ray diffraction for Na1. The second one is very mobile around its equilibrium position confirming the unexpected large thermal motion parameter observed for Na2. In any case, the isotropic chemical shift are close showing that the equilibrium position of Na2 is about the same as the Na1 one on the six-fold axis.

3.4. Thermal behavior

The thermal decomposition of the mixed oxalate was studied from TG measurements under airflow (Fig. 8) and TDXD (Fig. 9), from room temperature to 600°C. The chemical formula of the precursor found from the TG curve is $CdZrNa_2(C_2O_4)_4 \cdot 8.4H_2O$. The content in water molecules agrees well with that found from the crystal structure refinement. The decomposition of $CdZrNa_2(C_2O_4)_4 \cdot 8.4H_2O$ can be described as a three-step process. First, a weight loss is immediately observed on the TG curve when the product is heated from room temperature. The 10% weight loss observed between room temperature and the inflection point around 60°C corresponds to the departure of 4.4 water molecules. This result agrees well with the 10.5% weight loss, calculated for the departure of all less bonded water molecules (Ow2 and Ow3) located in the voids of the

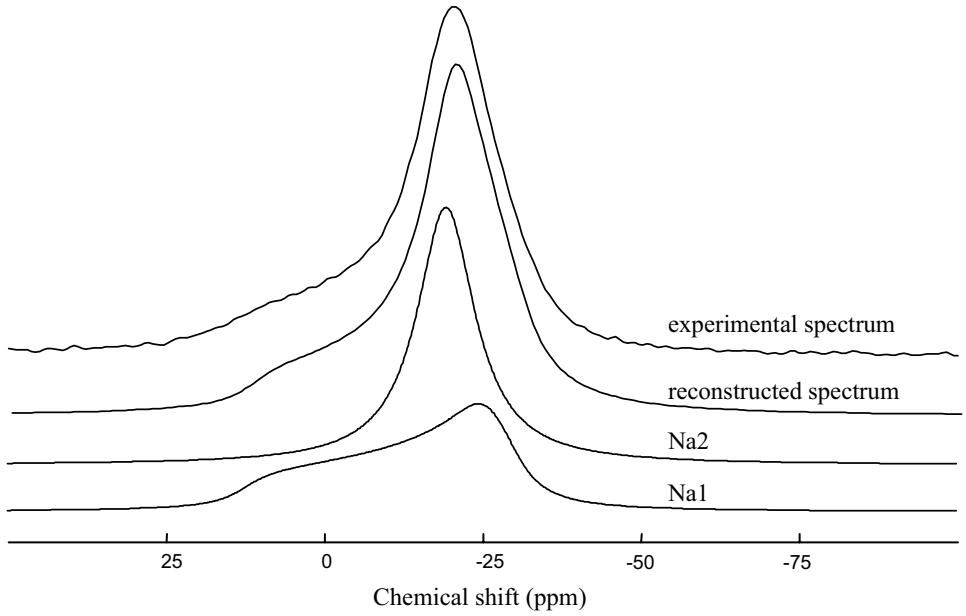

Fig. 7. ^{23}Na static spectrum evidencing two types of sodium atoms labeled Na1 and Na2.

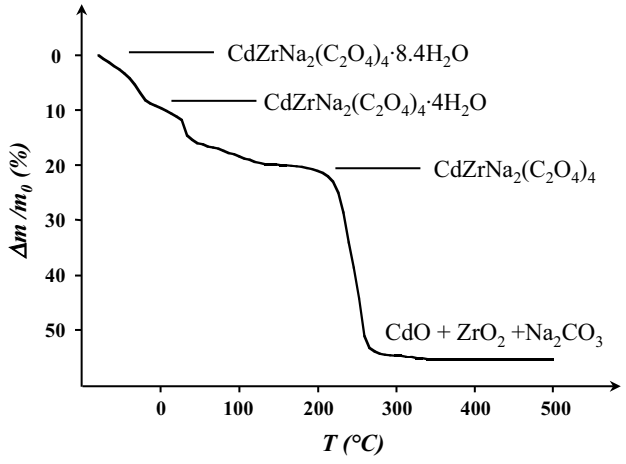

Fig. 8. TG curve for $CdZrNa_2(C_2O_4)_4 \cdot 8.4H_2O$ under flowing air (heating rate: $5°C\,h^{-1}$).

anionic framework. In this temperature range, the TDXD plot displays a slight shift of peak positions towards high angles. The departure of these less bonded water molecules is thus accompanied by a small contraction of the unit-cell parameters. The second step of the decomposition is the loss of the remaining water molecules found in the hexagonal cross section channels around the sodium atoms. This is shown by a subsequent 10% weight loss on the TG curve (calcd. 9.6%) between 60°C and 230°C. As seen from the TDXD plot, the loss of these water molecules leads to the formation of new phase stable between 50°C and 170°C that coexists with the precursor until 110°C. A plateau is then reached on the TG curve between 230 and 300°C, and an amorphous compound is observed in the temperature range 170–330°C on the TDXD plot. This plateau corresponds to the stability domain of the anhydrous ternary oxalate $CdZrNa_2(C_2O_4)_4$. The final weight loss (35%) agrees with the decomposition of the anhydrous phase into a mixture of cadmium oxide CdO, zirconium oxide ZrO_2 and sodium carbonate Na_2CO_3 (calcd. weight loss 32.4%). Indeed, the peaks of cubic CdO [PDF2 no. 75-0593] appear at ~300°C and those of tetragonal ZrO_2 [PDF2 no. 80-2156] at ~450°C [Powder Diffraction File, International Centre for Diffraction Data, Newton Square, PA]. It should be noted that the formation of amorphous sodium carbonate as already been reported in the previous studies, particularly in the decomposition of yttrium sodium oxalate [25].

4. Conclusion

The present study has clearly demonstrated that the new cadmium–zirconium–sodium oxalate adopts the structure type with an open anionic hexagonal framework. The monovalent element is located in the tunnels with a hexagonal cross section, together with water molecules. Both X-ray diffraction and NMR spectroscopy results have demonstrated the presence of two types of sodium atoms in the structure. The dynamic disorder observed from X-ray diffraction for sodium atoms and their surrounding water molecules has been confirmed by the high mobility of these entities described from the NMR results. The structure adopted by the sodium-based oxalate compound contrasts with that of the potassium analog in which K is eight-fold

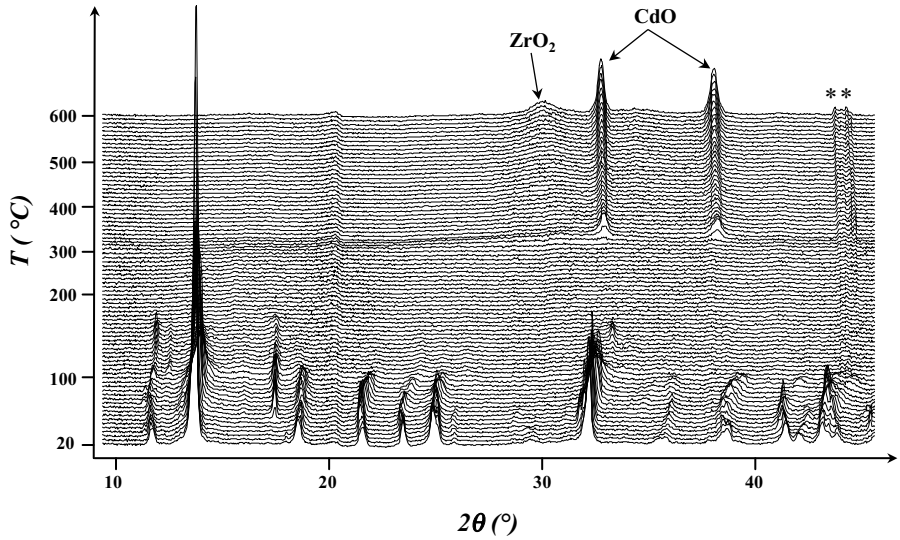

Fig. 9. TDXD plot for $CdZrNa_2(C_2O_4)_4 \cdot 8.4H_2O$ under flowing air (5°C h^{-1} between 20°C and 200°C and then 10°C h^{-1} until 600°C, counting time: 3600 s/pattern). * spurious diffraction lines due to the sample holder.

coordinated, with polyhedra displaying well-defined dodecahedra. It is interesting to note that the sodium atoms also have 'on average' an eight-fold coordination, with distorted polyhedra arising from the surrounding mobile water molecules Ow1. These polyhedra can be qualified as 'soft' with respect to the well-defined 'rigid' eight-fold Cd, Zr and K dodecahedra constituting the structure of the mixed oxalates adopting the 'square' structure type. The mobility of atoms in the NaO_8 polyhedra is a likely reason why the hexagonal structure type, already reported with ammonium and protonated ethylenediamine cations, is favored when sodium is used as a counter-cation.

Acknowledgments

The authors thank Dr. T. Roisnel (Centre de Diffractométrie X, Université de Rennes 1) and Mr. G. Marsolier for their assistance in single-crystal and powder X-ray diffraction data collection, respectively, and they are grateful to Mr. O. Rastoix (Centre de Microscopie Electronique à Balayage et microAnalyse, Université de Rennes 1) for SEM analysis.

References

[1] M. O'Keeffe, M. Eddaoudi, Hailian Li, T. Reineke, O.M. Yaghi, J. Solid State Chem. 152 (2000) 3.
[2] G. Férey, J. Solid State Chem. 152 (2000) 37.
[3] E. Jeanneau, N. Audebrand, J.-P. Auffrédic, D. Louër, J. Mater. Chem. 11 (2001) 2545.
[4] E. Jeanneau, N. Audebrand, D. Louër, Chem. Mater. 14 (2002) 1187.
[5] E. Jeanneau, N. Audebrand, D. Louër, J. Mater. Chem. 12 (2002) 1.
[6] J.L. Hoard, J.V. Silverton, Inorg. Chem. 2 (1963) 235.
[7] C.W. Haigh, Polyhedron 15 (4) (1996) 605.
[8] R.D. Shannon, C.T. Prewitt, Acta Crystallogr. B 25 (1996) 925.
[9] P. Bénard-Rocherullé, J. Rius, D. Louër, J. Solid State Chem. 21 (1997) 430.
[10] S.K. Kachroo, K.K. Bamzai, P.R. Dhar, P.N. Kotru, B.M. Wanklyn, Appl. Surface Sci. 156 (2000) 149.
[11] J. Plévert, J.P. Auffrédic, M. Louër, D. Louër, J. Mater. Sci. 24 (1989) 1913.
[12] P.P. Man, Appl. Magn. Reson. 4 (1993) 65.
[13] D. Massiot, F. Fayon, M. Capron, I. King, S. Le Calvé, B. Alonso, J-O. Durand, B., Bujoli, Z. Gan, G. Hoatson, Magn. Reson. Chem. 40 (2002) 70.
[14] Nonius, Kappa CCD Program Software, (Nonius BV, Delft, The Netherlands,) 1998.
[15] Z. Otwinowski, W. Minor, Methods Enzymol. 276 (1997) 307.
[16] P. Coppens, in: F.R. Ahmed, S.R. Hall, C.P. Huber (Eds.), Crystallographic Computing, Munksgaard Publishers, Copenhagen, 1970, pp. 255–270.
[17] K. Brandenburg, M. Berndt, Diamond (version 2.1e), Crystal Impact, Bonn, 2001.
[18] A. Altomare, M.C. Burla, M. Camalli, G. Cascarano, C. Giacovazzo, A. Guagliardi, A.G.G. Moliterni, G. Polidori, R. Spagna, J. Appl. Crystallogr. 32 (1999) 115.
[19] G.M. Sheldrick, SHELXL-97: programs for crystal structure refinement, University of Göttingen, Göttingen, 1997.
[20] C. Boudaren, J.P. Auffrédic, M. Louër, D. Louër, Chem. Mater. 12 (2000) 2324.
[21] I.D. Brown, J. Appl. Crystallogr. 29 (1996) 479.
[22] T. Hahn, Zeits. Kristallogr. 109 (1957) 438.
[23] A.L. Spek, Acta Crystallogr. Sect. A 46 (1990) C34.
[24] A. Abragam, Les principes du Magnétisme Nucléaire, Presses Universitaires de France, Paris, 1961, p. 223.
[25] T. Bataille, Ph.D. Thesis, University of Rennes, France, 2000.